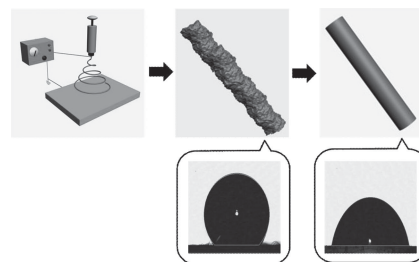


# Effect of Thermal Annealing on the Surface Properties of Electrospun Polymer Fibers

Jiun-Tai Chen,\* Wan-Ling Chen, Ping-Wen Fan, I-Chun Yao

Electrospun polymer fibers are gaining importance because of their unique properties and applications in areas such as drug delivery, catalysis, or tissue engineering. Most studies to control the morphology and properties of electrospun polymer fibers focus on changing the electrospinning conditions. The effects of post-treatment processes on the morphology and properties of electrospun polymer fibers, however, are little studied. Here, the effect of thermal annealing on the surface properties of electrospun polymer fibers is investigated. Poly(methyl methacrylate) and polystyrene fibers are first prepared by electrospinning, followed by thermal annealing processes. Upon thermal annealing, the surface roughness of the electrospun polymer fibers decreases. The driving force of the smoothing process is the minimization of the interfacial energy between polymer fibers and air. The water contact angles of the annealed polymer fibers also decrease with the annealing time.



## 1. Introduction

Electrospinning has been widely used to prepare polymer fibers with diameters ranging from several nanometers to a few micrometers.<sup>[1,2]</sup> Various types of polymer fibers have been fabricated by electrospinning for applications such as filtration,<sup>[3]</sup> catalysis,<sup>[4]</sup> wound dressing,<sup>[5]</sup> tissue engineering,<sup>[6]</sup> and drug delivery.<sup>[7]</sup> For different applications, the surface properties and morphologies of the electrospun polymer fibers play important roles. Most studies focus on controlling the surface properties and morphologies of electrospun polymer fibers by adjusting the experimental parameters during the electrospinning process. The experimental parameters include the polymer type, the polymer concentration, the flow rate, the working distance, and the applied voltage.<sup>[8]</sup> These parameters are crucial in obtaining electrospun fibers with unique

properties such as superhydrophobicity.<sup>[9]</sup> For examples, Jiang et al.<sup>[10]</sup> prepared porous microsphere/nanofiber composite films of polystyrene (PS) by electrospinning to mimic the topography of lotus leaves and to achieve a high water contact angle (WCA). The morphologies of the composite films were controlled by adjusting the concentration of the polymer solution. Superhydrophobicity (contact angle = 160.48°) was achieved because of the increasing surface roughness. Rutledge and co-workers<sup>[11]</sup> also prepared block copolymer poly(styrene-*b*-dimethylsiloxane) fibers in the range 150–400 nm by electrospinning. A contact angle of 163° and contact angle hysteresis of 15° were achieved due to the surface roughness of the electrospun fibers and the surface enrichment in siloxane.<sup>[11]</sup>

Despite many studies on controlling surface properties and morphologies of electrospun polymer fibers by adjusting electrospinning conditions, there have been only few studies on the effect of post-treatments on the surface properties and morphologies of electrospun polymer fibers. Post-treatments such as thermal annealing have been used for polymer bulks or polymer thin films. After annealing, polymer chains are mobile and can relax toward an equilibrium state.<sup>[12]</sup> Fong and

Prof. J. T. Chen, W. L. Chen, P. W. Fan, I. C. Yao  
Department of Applied Chemistry, National Chiao Tung  
University, Hsinchu, Taiwan 30050  
E-mail: jtchen@mail.nctu.edu.tw  
Tel: 886-3-5731631

co-workers<sup>[13]</sup> studied the crystalline morphology and polymorphic phase transitions of electrospun nylon-6 nanofibers by thermal annealing. Upon annealing above 150 °C, the metastable  $\gamma$ -crystals gradually melted and recrystallized into thermodynamically stable  $\alpha$ -form crystals. Tan and Lim<sup>[14]</sup> also studied the morphology change of electrospun poly(L-lactic acid) (PLLA) nanofibers by annealing. A purely fibrillar structure was changed to a mixture of fibrillar and nanogranular structures with enhanced interfibrillar bonding. The annealing process also causes the increase of the Young's modulus of the nanofiber because of the crystallinity.

In spite of these studies, the effect of thermal annealing on the surface morphologies and properties of electrospun polymer fibers is still not clear. For many applications in which annealing process is involved, it is always problematic to assume that the surface properties of the annealed fibers are equivalent to those of the unannealed fibers. Here, we investigate this effect by annealing electrospun fibers of two commonly used polymers, poly(methyl methacrylate) (PMMA) and PS. The surface morphologies of the as-spun polymer fibers are controlled by the electrospinning conditions. Upon thermal annealing, we find that the surface roughness of the electrospun fibers decreases, and the WCAs of the electrospun polymer fibers also decrease. After thermal annealing, the values of WCAs of polymer fibers are close to those of bulk polymer films. Rayleigh-instability-type transformation of the electrospun fibers, however, is not observed in this system.<sup>[15]</sup>

## 2. Experimental Section

### 2.1. Materials

Poly(methyl methacrylate) ( $\bar{M}_w$ : 75 kg mol<sup>-1</sup>) and PS ( $\bar{M}_w$ : 192 kg mol<sup>-1</sup>) were obtained from Sigma-Aldrich. *N,N*-dimethylformamide (DMF) was purchased from TEDIA.

### 2.2. Polymer Fibers by Electrospinning

The electrospinning processes were carried out using a vertical configuration at room temperatures. Polymer solutions with different concentrations were first prepared (PMMA: 25, 30, 35, and 40 wt%; PS: 20, 25, 30, and 35 wt%). In a typical electrospinning experiment to prepare PMMA fibers, for example, a 25 wt% of PMMA solution in DMF was added to a syringe, which was connected to a capillary nozzle (inner diameter: 0.41 mm). A syringe pump (KD Scientific) was used to feed the polymer solution into the capillary nozzle at a constant flow

rate of 0.1 mL h<sup>-1</sup>. The nozzle was connected to a high voltage power supply (SIMCO), and the range of the applied voltage was 10–30 kV. The working distance between the grounded collector and the capillary nozzle was 10–20 cm.

### 2.3. Thermal Annealing Processes of Polymer Fibers and Films

Electrospun PMMA and PS fibers were collected on glass substrates (1 × 1 cm<sup>2</sup>) and thermally annealed in an oven for different temperatures and times. Polymer films were prepared by blade coating or spin-coating techniques on glass substrates, followed by thermal annealing for different temperatures and times.

### 2.4. Structure Analysis and Characterization

The glass transition temperatures ( $T_g$ ) of PMMA and PS were measured by differential scanning calorimetry (DSC) (Seiko Instruments, EXSTAR 6000). The  $T_g$  of PMMA and PS used in this work are 110 and 109 °C, respectively. The surface morphologies of the polymer fibers before and after annealing were investigated by a scanning electron microscope (SEM) (JEOL, JSM-7401F) with an accelerating voltage of 10 kV. The samples were coated with 4 nm platinum before the SEM measurement.

## 3. Results and Discussion

Figure 1 shows the schematic illustration of the preparation of polymer fibers by electrospinning and the annealing treatment. The sizes and morphologies of the as-spun polymer fibers are controlled by adjusting

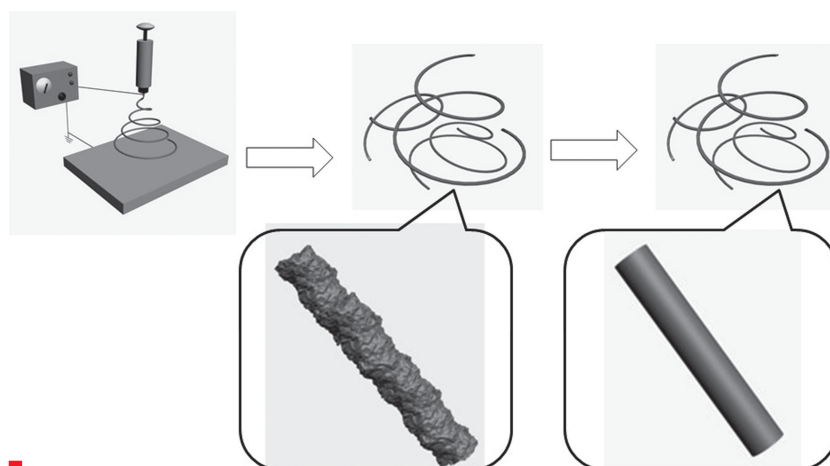


**Figure 1.** Schematic illustration of the electrospinning process to prepare polymer fibers and the thermal annealing process. After thermal annealing, the surface roughness of electrospun polymer fibers decreases. The water contact angles of the fibers also decrease upon thermal annealing.

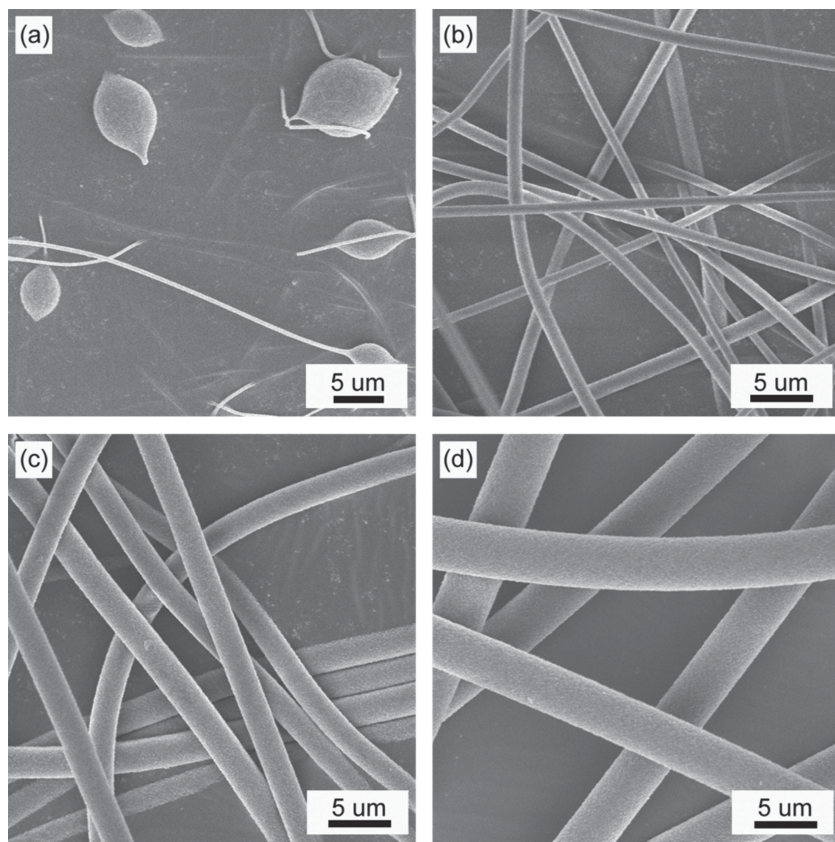


**Figure 2.** SEM images of PMMA ( $\overline{M}_w$ : 75 kg mol<sup>-1</sup>) fibers electrospun at different concentrations: a) 25, b) 30, c) 35, and d) 40 wt%. The applied voltage is 10 kV and the working distance is 15 cm. The feed rate is 1 mL h<sup>-1</sup>.

the electrospinning conditions including the polymer concentration, the flow rate, the working distance, and the applied voltage.<sup>[8]</sup> After the polymer fibers are collected, they are thermally annealed in an oven for different temperatures and times. The surface properties and morphologies of the samples annealed at different annealing conditions are examined by a scanning electron microscope and contact angle measurement.

Electrospinning is commonly used to prepare polymer fibers. With suitable solvents, almost all polymers can be prepared as fibers by this simple process. The aspect ratios of the electrospun polymer fibers are much larger than other one-dimensional polymer materials prepared by methods such as using anodic aluminum oxide templates.<sup>[16,17]</sup> In a typical electrospinning process, a polymer solution is prepared and fed into a capillary nozzle. The polymer solution is ejected from the nozzle at constant rates controlled by a syringe pump. The polymer solution is subjected to both the surface tension force and the electrostatic force established between the capillary nozzle and the ground collector. A conical shape of the solution droplet, referred to as the Taylor cone, with a half-angle of 49.3° is formed once the droplet is destabilized by the

electrostatic force.<sup>[18]</sup> With increasing the applied voltage, the electrostatic force can overcome the surface tension force of the droplet, resulting in the formation of a charged jet of polymer solution. The solution jet is further thinned by the bending instability.<sup>[19]</sup> Finally, polymer fibers are obtained and collected after the fast evaporation of the solvent.

The morphologies and sizes of the polymer fibers can be simply controlled by the electrospinning conditions, such as the polymer concentration, the flow rate, the working distance, and the applied voltage. One of the most common ways to control the morphologies and sizes of electrospun fibers is by adjusting the polymer concentration.<sup>[20]</sup> In general, the diameter of the electrospun fibers increases with the polymer concentration because of the increased solution viscosity. Tan and co-workers<sup>[21]</sup> studied that the fiber diameter increases with the solution concentration according to a power law relationship. Figure 2 shows the SEM images of PMMA ( $\overline{M}_w$ : 75 kg mol<sup>-1</sup>) fibers electrospun at different concentrations while keeping other experimental parameters constant. The

concentration of PMMA in DMF is changed from 25 to 40 wt% with the feed rate of 1 mL h<sup>-1</sup>. The applied voltage is 10 kV and the working distance is 15 cm. At 25 wt%, beads-on-string structures are observed, as shown in Figure 2a. The formation of the beaded fibers is caused by both the entanglement of the polymer chains and the contraction of the radius of the solution jet driven by the surface tension.<sup>[22]</sup> With higher solution concentration, the sizes of the beads become bigger, and the distances between beads are longer. Fibers without beads can finally be formed once a critical polymer concentration is reached. The diameters of the electrospun PMMA fibers are increased from  $\approx 1$ – $1.5 \mu\text{m}$  for 30 wt% to  $\approx 4$ – $4.5 \mu\text{m}$  for 40 wt%, as shown in Figure 2b,c, and d. Although fibers with larger diameters can be prepared by using even higher polymer concentrations, the polymer solution might be too viscous to be ejected from the capillary nozzle once the concentration is too high.

The dependency of fiber diameters on the polymer concentration can also be seen for PS fibers. Figure S1 (Supporting Information) shows the SEM images of PS ( $\overline{M}_w$ : 192 kg mol<sup>-1</sup>) fibers electrospun at different concentrations while keeping other experimental parameters



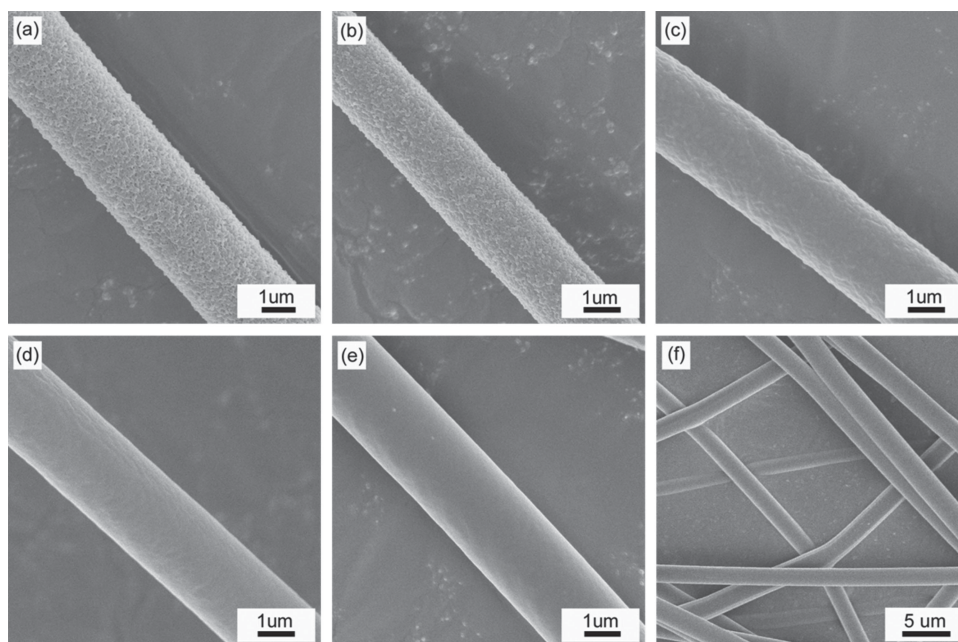


Figure 3. SEM images of electrospun PMMA fibers annealed at 130 °C for different times: a) 0, b) 5, c) 10, d) 30, e, f) 90 min at different magnifications.

constant. The concentration of PS in DMF is changed from 20 to 35 wt% with the feed rate of 1 mL h<sup>-1</sup>. The applied voltage is 10 kV, and the working distance is 15 cm. The diameters of the electrospun PS fibers are increased from ≈2–3 μm for 20 wt% to ≈5–5.5 μm for 35 wt%, as shown in Figure S1a–d (Supporting Information).

Other than polymer concentration, the sizes of the electrospun fibers can also be controlled by other electrospinning parameters. For example, the fiber diameters can be controlled by changing the feed rate. The diameter of the electrospun fibers increases with the feed rate. In addition, fibers with larger diameters can be prepared by using a lower applied voltage because of the lower electric field.<sup>[23]</sup>

After the preparation of electrospun polymer fibers, the fibers are collected and annealed in an oven for different temperatures and times. For PMMA, we choose the fibers made from 35 wt% of PMMA ( $\bar{M}_w$ : 75 kg mol<sup>-1</sup>) in DMF with an applied voltage of 10 kV and a feed rate of 1 mL h<sup>-1</sup>. Under this condition, PMMA fibers without beaded structures are prepared. The diameters of PMMA fibers prepared by this condition are ≈5–5.5 μm. Figure 3 shows the SEM images of electrospun PMMA fibers annealed at 130 °C for different times. Before annealing, the surface of the as-spun fiber is rough (see Figure 3a). After annealing, the surface roughness decreases gradually. By annealing at 130 °C for 30 min, the surface of the fiber becomes smooth. But the fibrillar shape of the fiber is still maintained, as shown in Figure 3f with a lower magnification. At higher annealing temperatures (150 °C), similar smoothing

process is observed, as shown in the Supporting Information. But the time for the surface of the fiber to become smooth is shorter. In addition, the fibers melt together with other fibers, as shown in Figure S2f (Supporting Information) with a lower magnification. When the annealing temperature is increased to 170 °C, the smoothing process is even faster.

The optimal condition for annealing the electrospun PMMA fibers without forming melted films is at a lower temperature (130 °C) for 0 to 90 min. To avoid the formation of porous films by thermal annealing at higher temperature, one possible way is to anneal the electrospun polymer fibers in a uniform environment. For example, the fibers can be dispersed and thermally annealed in a nonsolvent such as ethylene glycol. During the annealing process, the stirring process can avoid the aggregation of the polymer fibers.<sup>[24]</sup> For as-spun PS fibers, the smoothing process is similar when the fibers are annealed at different temperatures. After annealed at higher temperatures (170 °C) annealing, fibers melt together and form a porous film structure.

In this work, the roughness change of the electrospun polymer fibers is demonstrated qualitatively from the SEM images. A quantitative analysis on the roughness change from the SEM data is difficult because of the curved surface of the polymer fibers. The quantitative surface analysis may be performed by using special softwares such as Mex 3D (Alicona Imaging GmbH). Using these softwares, SEM images taken at different tilt angles can be mathematically processed, and three-dimensional SEM images can be reconstructed.

Here, we focus on the surface morphology and properties of polymer fibers away from the substrate, and the substrate effect is not considered. For polymer fibers in contact with the substrate, wetting or dewetting on the substrate might occur after thermal annealing. Previously, we studied that electrospun PS fibers can wet the glass substrate after thermal annealing.<sup>[15]</sup> We also found that a Rayleigh-instability-driven morphology transformation can be observed when the electrospun PS fibers are annealed on a PMMA-coated substrate. The polymer fibers transform into hemispherical polymer particles, caused by the lower surface tension of PS than that of PMMA and the interfacial tension between PS and PMMA.<sup>[15]</sup> Here, however, many layers of electrospun fibers on substrates are prepared, and the substrate effect is neglected.

In addition to study the surface morphologies of electrospun fibers by SEM, the annealed electrospun polymer fibers are examined by WCA measurement. The roughness of a solid surface can significantly affect the contact angle and the contact angle hysteresis.<sup>[25]</sup> For a smooth surface, the contact angle is determined by the Young's equation:

$$\gamma_{SA} = \gamma_{SL} + \gamma \cos \theta \quad (1)$$

where  $\theta$  is the contact angle, and  $\gamma_{SA}$ ,  $\gamma_{SL}$ , and  $\gamma$  are the surface tensions of solid/air, solid/liquid, and liquid/air, respectively.<sup>[26]</sup> The surface is referred to as hydrophilic when the contact angles lie between  $0^\circ$  and  $90^\circ$  and as hydrophobic when the contact angles lie between  $90^\circ$  and  $180^\circ$ . The effect of roughness on the contact angles is first appreciated by Wenzel, who used a geometrical

argument.<sup>[27]</sup> The change of contact angles can be predicted by the Wenzel relation:

$$\cos \theta^* = r \cos \theta, \quad (2)$$

where  $r$  is the roughness factor, defined by the ratio between the actual surface area and the projected surface area. If the roughness factor is larger than 1, a hydrophobic surface becomes more hydrophobic, and a hydrophilic surface becomes more hydrophilic.<sup>[25]</sup> Cassie and Baxter later used another equation to predict the contact angle of a binary composite which contains two components:

$$\cos \theta = f_1 \cos \theta_1 + f_2 \cos \theta_2 \quad (3)$$

where  $\theta_1$  and  $\theta_2$  are the contact angles of the two components, and  $f_1$  and  $f_2$  are the area fractions of the two components.<sup>[28]</sup> Therefore, the roughness change of the electrospun polymer fibers is expected to cause the change of WCAs.

Figure 4a–c shows the plot of WCA of electrospun PMMA fibers annealed at 130, 150, and 170 °C. It has been studied that the WCAs of as-spun fibers depend on the sizes of the electrospun fibers. For example, Rutledge and co-workers<sup>[20]</sup> studied that the hydrophobicity increases monotonically up to a contact angle of  $\approx 155^\circ$  with a reduction of fiber diameters by using initiated chemical vapor deposition (iCVD)-coated poly(caprolactone) (PCL) fibers.<sup>[20]</sup> They found that the contact angles for both bead-free fibers and beaded fibers increase as the average fiber diameter decreases. Therefore, we use polymer fibers prepared under the same electrospinning conditions for the annealing studies to obtain polymer fibers with similar diameters and initial WCAs. Still, the size distribution

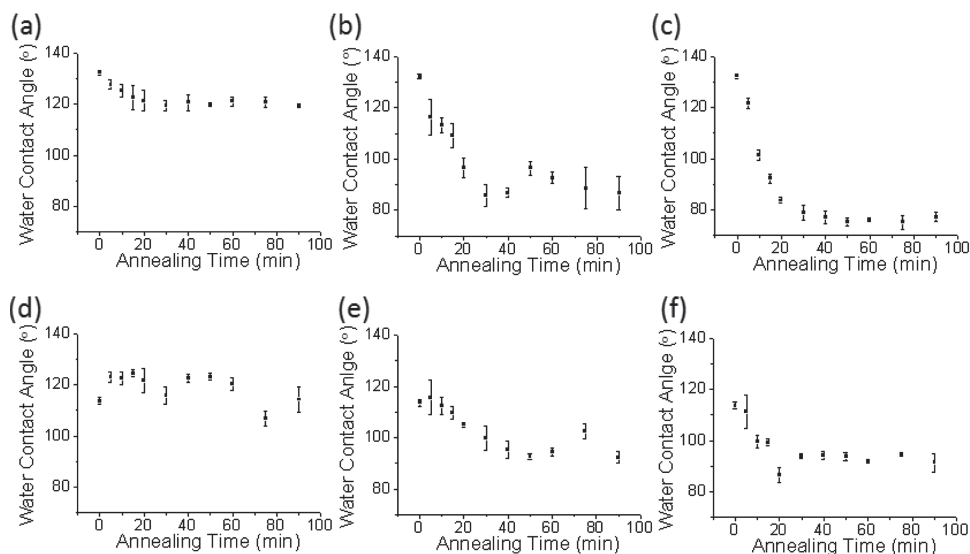


**Figure 4.** a–c) The plot of water contact angle of electrospun PMMA fibers annealed at 130 (a), 150 (b), and 170 °C (c). d–f) The plot of water contact angle of electrospun PS fibers annealed at 130 (d), 150 (e), and 170 °C (f).

of the as-spun fibers can result in the deviations in the data of WCA measurement. In addition, the arrangement of the fibers on the substrate also causes deviations in the data. Before thermal annealing, the contact angle is  $\approx 135^\circ$ . When the annealing temperature is  $130^\circ\text{C}$ , the contact angle only decreases slightly and is maintained at around  $120^\circ$  with annealing time, even though the surface of the fiber surface becomes smooth. For the samples annealed at  $150^\circ\text{C}$ , the contact angle decreases gradually with time and reaches  $\approx 75^\circ$  for the annealing time from 30 to 90 min. When the annealing temperature is increased to  $170^\circ\text{C}$ , the WCA decreases at a faster rate than those annealed at  $130$  or  $150^\circ\text{C}$ . After annealing at  $170^\circ\text{C}$  for  $\approx 20$  min, the WCA decreases quickly from  $\approx 135^\circ$  to  $\approx 85^\circ$  and maintains at  $\approx 75^\circ$  at longer annealing time, which is close to the WCA of a bulk PMMA film.

WCA measurements are also performed for electrospun PS fibers. The contact angles of the as-spun PS fibers are  $\approx 115^\circ$ . After annealing, similar trend in WCAs is observed for electrospun PS fibers. The WCA of electrospun PS decreases upon thermal annealing, as shown in Figure 4e–f. By annealing at  $170^\circ\text{C}$  for 30 min, for example, the WCA decreases from  $\approx 115^\circ$  to  $\approx 95^\circ$ . Similar to the case of PMMA fibers, the decreasing rate in WCAs of PS fibers is higher at higher annealing temperatures. After annealing for longer time, the WCA of PS fibers is close to that of a bulk PS film ( $\approx 95^\circ$ ).

For amorphous polymers, the thermal annealing process is usually performed above the  $T_g$  of the polymers. The  $T_g$  of PMMA and PS used in this work is measured to be  $110$  and  $109^\circ\text{C}$ , respectively. There have been studies about the surface and interface effect on the elevation or reduction of  $T_g$  in polymers.<sup>[29]</sup> Here, however, we only consider the  $T_g$  values of bulk polymers. But the  $T_g$  values of polymer chains near the surface of the electrospun polymer fibers might be different from the  $T_g$  values of polymer chains near the core of the polymer fibers.

The roughness change of the electrospun polymer fibers can result in other property changes of the polymer fibers. For example, Kaneko and co-workers<sup>[30,31]</sup> studied that the absorption of polycyclic aromatic hydrocarbons on single wall carbon nanotubes is strongly affected by the nanoscale curvature effect. They found that tetracene adsorption was more than six times greater than that of phenanthrene. Therefore, the nanoscale curvatures on the rough polymer fibers varied by annealing can result in different absorption abilities of organic molecules. In addition, the information about the roughness change of the polymer fibers can be useful for separation membranes based on molar mass fractionation.<sup>[32]</sup>

After annealing, the surface changes from rough to smooth. The driving force for the reduction in roughness is to reduce the surface area between polymer and air. This result can be compared with our previous study

of annealing electrospun polymer fibers in contact with nanoporous anodic aluminum oxide templates.<sup>[33]</sup> After the annealing process, the polymer chains wet the nanopores of the templates and form hierarchical polymer structures on the polymer fibers. The high surface energy of the pore walls of the aluminum oxide templates causes the wetting of polymer melts by capillary force.

Previously, we also studied the Rayleigh-instability-type transformation of electrospun PMMA fibers by thermally annealing the fibers in ethylene glycol, a non-solvent for the polymer.<sup>[24]</sup> The surface of polymer fibers undulates with a finite wavelength to reduce the interfacial area between fiber and ethylene glycol. The undulation grows with time, and polymer fibers transform into polymer spheres with sizes determined by the original diameters of the polymer fibers. The driving force for the transformation is the minimization of the interfacial energy between polymers and ethylene glycol.<sup>[34,35]</sup> This type of instability, however, is not observed when the as-spun polymer fibers are annealed in air, as we demonstrate here. The absence of the undulation of the fiber surface might be caused by the following reasons: First, the viscosity ratio between the polymer and air is much higher than that between the polymer and ethylene glycol.<sup>[36]</sup> Therefore, the driving force is not enough to induce the structure transformation due to kinetic consideration. Second, the polymer fibers are in contact with other fibers during the annealing process. We expect that the transformation of electrospun polymer fibers to polymer spheres can occur if the polymer fibers are embedded in another polymer matrix.

The initial roughness of electrospun polymer fibers is mainly controlled by the electrospinning conditions, such as the type of polymer, the solvent, the humidity, the flow rate, or the working distance. In this work, we study the roughness change of electrospun fibers with high initial roughnesses. For many electrospun fibers with low initial roughnesses, this work also provides useful information for the decrease of roughness by annealing treatments, which is often ignored.

## 4. Conclusion

We study the effect of thermal annealing on the surface properties and morphologies of electrospun PMMA and PS fibers. After thermal annealing, the surface roughness of the electrospun polymer fibers decreases. The WCAs of PMMA fibers decrease from  $\approx 135^\circ$  to  $\approx 75^\circ$ , which is close to the WCA of a bulk PMMA film. Similarly, the WCAs of PS fibers also decrease from  $\approx 115^\circ$  to  $\approx 95^\circ$ , which is close to the WCA of a bulk PS film. This work not only provides a simple approach to control the surface properties of electrospun polymer fibers but also contributes to a better

understanding of the relationship between the contact angle and the surface roughness of polymer fibers.

## Supporting Information

Supporting Information is available from the Wiley Online Library or from the author.

Acknowledgements: This work was supported by the National Science Council.

Received: March 25, 2013; Revised: April 23, 2013; Published online: May 31, 2013; DOI: 10.1002/marc.201300290

Keywords: annealing; contact angle; electrospinning; nanofibers; polymers

- [1] A. Greiner, J. H. Wendorff, *Angew. Chem. Int. Ed.* **2007**, *46*, 5670.
- [2] D. Li, Y. N. Xia, *Adv. Mater.* **2004**, *16*, 1151.
- [3] S. Agarwal, J. H. Wendorff, A. Greiner, *Polymer* **2008**, *49*, 5603.
- [4] X. F. Lu, C. Wang, Y. Wei, *Small* **2009**, *5*, 2349.
- [5] D. Liang, B. S. Hsiao, B. Chu, *Adv. Drug Delivery Rev.* **2007**, *59*, 1392.
- [6] A. Martins, J. V. Araujo, R. L. Reis, N. M. Neves, *Nanomedicine* **2007**, *2*, 929.
- [7] E. R. Kenawy, F. I. Abdel-Hay, M. H. El-Newehy, G. E. Wnek, *Mater. Chem. Phys.* **2009**, *113*, 296.
- [8] A. Frenot, I. S. Chronakis, *Curr. Opin. Colloid Interface Sci.* **2003**, *8*, 64.
- [9] K. Acatay, E. Simsek, C. Ow-Yang, Y. Z. Menceloglu, *Angew. Chem. Int. Edit.* **2004**, *43*, 5210.
- [10] L. Jiang, Y. Zhao, J. Zhai, *Angew. Chem. Int. Ed.* **2004**, *43*, 4338.
- [11] M. L. Ma, R. M. Hill, J. L. Lowery, S. V. Fridrikh, G. C. Rutledge, *Langmuir* **2005**, *21*, 5549.
- [12] I. M. Hodge, A. R. Berens, *Macromolecules* **1982**, *15*, 762.
- [13] Y. Liu, L. Cui, F. X. Guan, Y. Gao, N. E. Hedin, L. Zhu, H. Fong, *Macromolecules* **2007**, *40*, 6283.
- [14] E. P. S. Tan, C. T. Lim, *Nanotechnology* **2006**, *17*, 2649.
- [15] P. W. Fan, W. L. Chen, T. H. Lee, Y. J. Chiu, J. T. Chen, *Macromolecules* **2012**, *45*, 5816.
- [16] M. F. Zhang, P. Dobriyal, J. T. Chen, T. P. Russell, J. Olmo, A. Merry, *Nano Lett.* **2006**, *6*, 1075.
- [17] C. W. Lee, T. H. Wei, C. W. Chang, J. T. Chen, *Macromol. Rapid Commun.* **2012**, *33*, 1381.
- [18] G. Taylor, *Proc. R. Soc. London, Ser. A* **1969**, *313*, 453.
- [19] D. H. Reneker, A. L. Yarin, H. Fong, S. Koombhongse, *J. Appl. Phys.* **2000**, *87*, 4531.
- [20] M. L. Ma, Y. Mao, M. Gupta, K. K. Gleason, G. C. Rutledge, *Macromolecules* **2005**, *38*, 9742.
- [21] J. M. Deitzel, J. Kleinmeyer, D. Harris, N. C. B. Tan, *Polymer* **2001**, *42*, 261.
- [22] H. Fong, I. Chun, D. H. Reneker, *Polymer* **1999**, *40*, 4585.
- [23] C. Wang, C. H. Hsu, J. H. Lin, *Macromolecules* **2006**, *39*, 7662.
- [24] P. W. Fan, W. L. Chen, T. H. Lee, J. T. Chen, *Macromol. Rapid Commun.* **2012**, *33*, 343.
- [25] D. Quere, in *Annual Review of Materials Research*, Annual Reviews, Palo Alto **2008**, p. 71.
- [26] T. Young, **1805**, *313*, 65.
- [27] R. N. Wenzel, **1936**, *28*, 988.
- [28] A. B. D. Cassie, S. Baxter, **1944**, *40*, 546.
- [29] J. L. Keddie, R. A. L. Jones, R. A. Cory, *Faraday Discuss.* **1994**, *98*, 219.
- [30] S. Gotovac, H. Honda, Y. Hattori, K. Takahashi, H. Kanoh, K. Kaneko, *Nano Lett.* **2007**, *7*, 583.
- [31] T. Ohba, T. Matsumura, K. Hata, M. Yumura, S. Lijima, H. Kanoh, K. Kaneko, *J. Phys. Chem. C* **2007**, *111*, 15660.
- [32] A. Lehtinen, R. Paukkeri, *Macromol. Chem. Phys.* **1994**, *195*, 1539.
- [33] J. T. Chen, W. L. Chen, P. W. Fan, *ACS Macro Lett.* **2012**, *1*, 41.
- [34] J. T. Chen, M. F. Zhang, T. P. Russell, *Nano Lett.* **2007**, *7*, 183.
- [35] D. Chen, J. T. Chen, E. Glogowski, T. Emrick, T. P. Russell, *Macromol. Rapid Commun.* **2009**, *30*, 377.
- [36] P. H. M. Elemans, J. M. H. Janssen, H. E. H. Meijer, *J. Rheol.* **1990**, *34*, 1311.